Conveying Characteristics of Dual Pneumatic Feeder Used for Biomass Pyrolysis

Xiao Wang and Hui Si *

A novel dual pneumatic feeder was developed to achieve constant and steady biomass conveying for pyrolysis. To facilitate the feedstock replenishment, an injection pipe was installed inside a pressure chamber to convey the feedstock. Another stream of gas entered the pressure chamber from the bottom to fluidize the particles. Experiments were performed to test the performance of the new feeder, and three injection pipes and gas distributors were used. Results showed that the feeding rate depended on both the injection and fluidizing gas velocities. The feeding rate decreased with the inner diameter (ID) of an injection pipe, due to its impact on gas velocity, while the effective injection distance had a negative effect within a certain range. The opening ratio of the gas distributors had a positive effect on the feeding rate. Then, a model was developed, based on the Ergun equation, to describe relationships between the feeding rate and the gas velocities. The classical equation was further reformed to establish the correlation between the solid mass flowrate and the construction parameters of the feeder. The developed model deviated from the measured values within ± 15%, which was considered capable to predict the feeder performances.

Keywords: Biomass feeder; Pneumatic conveying; Horizontal pipe; Injection pipe; Modeling; Pyrolysis

*Contact information: School of Technology, Beijing Forestry University, No. 35 Tsinghua East Road, Haidian District, Beijing, China; *Corresponding author: sihui@bjfu.edu.cn*

INTRODUCTION

Biomass is a renewable energy resource that can be used to reduce greenhouse gas emissions for environmental issues. Among all conversion approaches, pyrolysis of biomass has become the most prevalent method for liquid fuel production to address energy and environmental problems (Luo *et al*. 2016a). It has been found that pyrolysis of woody biomass, especially pinewood, results in higher liquid product yield (Luo *et al*. 2016b). Woody biomass is hygroscopic, which has a significant impact on the flowability. As a result, woody biomass feeding becomes a challenging step in pyrolysis progress, where the feedstock has to be rapidly and stably transported without interruption (Campbell *et al*. 2012; Dai *et al*. 2012). There are two forms of feeding available for biomass solids: mechanical and pneumatic feeding. Mechanical feeders tend to limit themselves to medium scale systems, due to the speed limitation and abrasion (Suri and Horio 2009). Pneumatic feeders are fit to large-scale systems and are successfully used in a variety of industries including chemical, mining, agriculture, and food. Wypych (1999) has reviewed typical blow tank designs, which handle a wide range of products in practical applications. However, conveying characteristics of woody biomass particles is quite different from that of other particles such as coal and ash, due to their higher moisture content and lower density (Dai *et al*. 2012). These caused serious bridging or agglomeration, leading to failure

in use of such pneumatic feeders. To increase the conveying stability, a fluidized bed was used as a conveying device to improve the flowability of biomass particles.

The utilization of a fluidized bed for the particle conveying can be dated back to 1959, at which time the method was shown to be much more efficient than traditional pneumatic conveying devices (Wen and Simon 1959). Then Massimilla *et al*. (1961) investigated the solids efflux from the fluidized bed through an orifice. They observed that the flow rate of solids depended on the diameter of the orifice and the efflux pressure, while the fluidizing gas velocity had a slight influence. Tallon, Woods, and coworkers developed models to predict the solids discharge rate from the fluidized beds (Tallon and Davies 2005; Woods *et al*. 2008; Watson *et al.* 2012). They also successfully used a pressurized bed of fluidized particles to convey solids vertically. Moreover, there were many other types of feeder construction that have been considered. Pugsley *et al.* (1996) replaced the traditional standpipe of the circulating fluidized bed riser with an aerated annular bed, which immersed the orifices of the riser to achieve very high and carefully controllable solids mass fluxes. Annamalai *et al*. (1992) proposed a locally fluidizing feeder that involved only local fluidization around the off-take pipe, rather than the fluidization of the whole bed. This concept was also adopted by Suri and Horio (2009), who located a vertical tube at the center of the distributor for particles discharging. The bottom of the vertical tube was connected with a horizontal pipe for particles transport.

However, most of these feeders were used for conveying charcoal and chemicals, which had nearly no water content. Because of the higher moisture content, woody biomass particles tend to be more viscous than other particles, leading to the high risk of being blocked up in the off-take of the fluidized bed when being discharged. Only a limited amount of information has been published on biomass feeding for pyrolysis. Therefore, more attention was devoted to the biomass feeder design. A new type of a dual pneumatic conveying feeder was developed, which combined the advantages of Pugsley's and Suri's design concepts to provide a constant and stable biomass particle conveying for pyrolysis. A closed pressure chamber was designed to contain biomass just like Suri's cartridge feeder. Instead of using a vertical discharge tube, a horizontal feeding pipe was installed at one side the pressure chamber. Another pipe, used for gas injection, was installed inside the pressure chamber coaxial with the feeding pipe, so that it would be immersed in biomass particles just like the mode of Pugsley's feeder. To avoid bridging or agglomeration, a distributor was also set inside the pressure chamber just below the feeding pipe to achieve particles fluidization. With such a gas injection pipe immersed in biomass particles, the particles would be picked up and conveyed by the gas more easily. Once the particles were removed, a gap would be formed instantaneously near the exit of the pipe, leading to the local pressure decrease, as a result, the ambient particles would replenish the gap immediately. Also, using the injection pipe would shorten the distance where gas traveled inside the pressure chamber. Meanwhile, the gas would be introduced through the distributor from another pipeline to improve the particles flowability instead of full fluidization. The distinguishing features of the dual pneumatic feeder developed in this study lies in its improvement in biomass flowability, simple construction, and lower energy consumption.

The objective of the present work was to test the conveying characteristics of this dual pneumatic feeder. Both effects of dual gas flows and construction parameter on feeder performance were studied. Then, a mathematical model was developed to describe the conveying mechanism inside the feeder, which can be applied for biomass feeder design.

EXPERIMENTAL

Materials

The biomass used in this study was masson pine, ground to particle size, and the size distribution is shown in Table 1. The bulk density, voidage, and moisture content of the larch particles were 210 kg/m^3, 70%, and 10.3 wt.%, respectively.

Table 1. Particle Size Distribution of Feedstock

Particle Size (mm)	< 0.15	0.15 to 0.22	0.22 to 0.355	0.355 to 0.50	0.50 to 0.60	0.60 to 0.75	> 0.75
Range (%)	1.0	0.6	25.7	22.4	14.1	18.2	18.0

Methods

The experimental equipment used to test the performance of the dual pneumatic feeder is shown in Fig. 1. The feeder consisted of a hopper, pressure chamber, butterfly valve, injection pipe, gas distributor, and a feeding pipe. The pressure chamber used to contain the feedstock was a stainless steel cylinder of 200 mm inner diameter (ID) and 350 mm in length with a feeding pipe horizontally located at one side. The feeding pipe was made of a 0.5 inch stainless steel pipe with a plexiglass section to observe the internal situation. A clamping sleeve was mounted on the other side of the pressure chamber to change and adjust the injection pipe. Three injection pipes with different ID, (9.5 mm, 13.5 mm, and 16.5 mm), with 300 mm in length were used in this study to investigate their effects on biomass particle conveying. The gas distributor was installed inside the pressure chamber to facilitate the feedstock fluidization to avoid bridging and agglomeration. Also, three gas distributors with 2-mm holes and different arrangements were used in this study to investigate their effects, as shown in Fig. 2. It was noteworthy that the gas distributor C, where holes were non-uniformly arranged, had a higher opening ratio on one half while a lower opening ratio on the other half to further study the effect of the hole arrangement on the conveying performance. The butterfly valve was installed between the hopper and the pressure chamber to guarantee the pressure of the pressure chamber during conveying. It could not be opened until the pressure chamber was empty.

An air pump was used to provide the feeder with the injection and fluidizing gas and was connected with a surge vessel of about 0.5 m^3 in volume. The surge vessel was used to stabilize the pressure, which was maintained at 20 kPa. There were two outlets set on the surge vessel to connect to the injection pipe and the bottom of the pressure chamber for providing the injection and fluidizing gas, respectively. Also, two rotor flow meters were used to monitor the volume flow rates, which were controlled by ball valves.

The objective of the experiment was to investigate the influences of operating and construction parameters that included the velocities of injection, fluidizing gas, injection pipes, and gas distributors on the performance of the feeder. In each run of the experiment, the feedstock was collected from the feeding pipe and was measured by an electronic balance to calculate the solid mass flow rate to represent the feeding rate, as shown in Fig. 1. Each single run would be repeated 12 times to get the mean value of the mass flow rate to obtain reasonable analysis results. Standard deviations would be also calculated which was correlated with feeding fluctuation to measure the stability of biomass conveying.

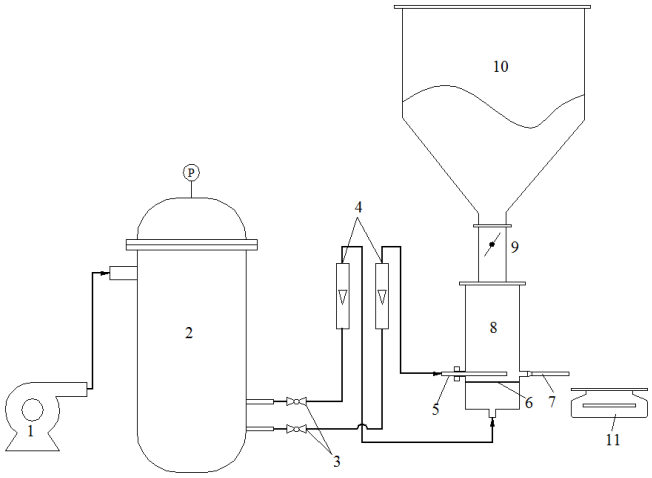

Fig. 1. Schematic diagram of experimental equipment of dual pneumatic feeder; (1) Air pump; (2) Surge vessel; (3) Ball valves; (4) Rotor flow meters; (5) Injection pipe; (6) Gas distributor; (7) Feeding pipe; (8) Pressure chamber; (9) Butterfly valve; (10) Hopper; and (11) Electronic balance

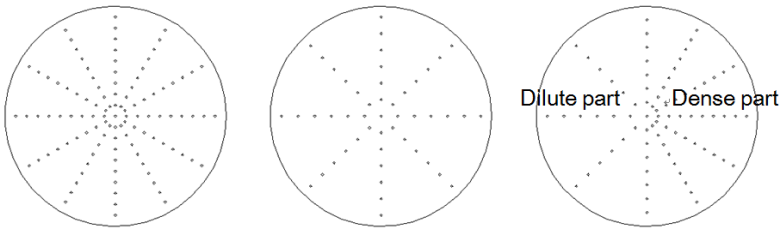

Fig. 2. Gas distributors with different hole arrangements used in experiment; A. opening ratio 1.09%, uniform arrangement; B. opening ratio 0.45%, uniform arrangement; and C. opening ratio 0.78%, non-uniform arrangement

RESULTS AND DISCUSSION

Effect of Gas Velocity on Biomass Feeding

The effect of the injection gas velocity was investigated by fixing the fluidizing gas flowrate ($m_{g,fl}$) to 0. The experiment was performed using a gas distributor (A) and 9.5 mm ID injection pipe 50 mm away from the feeding pipe (L = 50 mm). The variation of the feeding rate (m_s) along with the standard deviation with the injection gas velocity ($v_{g,in}$) are plotted in Fig. 3. The solid to gas flowrate ratios $\left(m_s/m_g, m_g = m_{g,in} + m_{g,fl}\right)$ were also calculated. As shown, with the increase in $v_{g,in}$, the feeding rate increased while the standard deviation tended to decrease (from 0.0011 to 0.0004). This showed that the stability of the biomass particles movement was improved by increasing gas velocity in the feeding pipe. According to a visual observation through the transparent section of the feeding pipe, the biomass particles deposited in the bottom of the pipe increased with reduced gas velocity, which led to a transition from a suspension to a strand flow that caused fluctuation in conveying. A similar result was found by Wypych and Yi (2003). The solid to gas flowrate ratio did not decrease with the injection gas velocity, until the peak value of $v_{g,in}$ was achieved around 6 m/s. Also, few solids were observed in the bottom of the feeding pipe when $v_{g,in}$ reached 6 m/s, which indicated that the principle of improving conveying

efficiency in a horizontal pipe was to pick up deposited solids until all of them were suspended in moving gas. However, if $v_{g,in}$ increased beyond the peak value, the feeding rate would not increase remarkably, since there were not enough solids stored in the feeding pipe, which resulted in a decreased m_s/m_g.

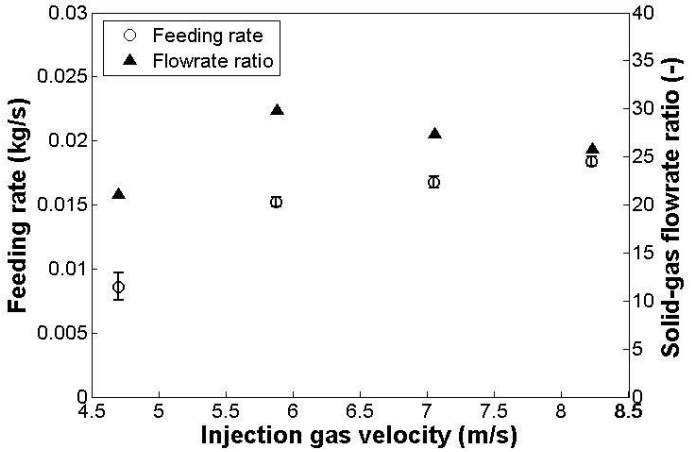

Fig. 3. Feeding rate as a function of injection gas velocity ($m_{g,fl}$ = 0, L = 50 mm, injection nozzle ID 9.5 mm, gas distributor A)

Then, the effect of the fluidizing gas was studied by fixing $m_{g,in}$ to 0. As shown in Fig. 4, both m_s and m_s/m_g increased with $v_{g,fl}$. It seemed that the effect of $v_{g,fl}$ was more remarkable than $v_{g,in}$ since velocities of fluidizing gas used for conveying were much lower than that of injection gas according to the comparison of Figs. 3 and 4. However, m_s/m_g was much lower than that in cases where only the injection gas was used, which was attributed to the kinetic energy dissipation caused by the gas distributor and biomass particles fluidization. Standard deviations (aroud 0.0004) were smaller than those in Fig. 3, and the feeding fluctuation calculated did not exceed $\pm$5%. This showed that the fluidizing gas helped to achieve the constant and stable conveying.

The conveying characteristics using both injection and fluidizing gas were studied, and the results are shown in Figs. 5 and 6. The feeding rates were improved dramatically compared with that in Figs. 3 and 4. However, m_s/m_g tended to decrease with gas velocity. This was attributed to the fact that the total gas flowrate was already high enough to make all solids become suspended in moving gas. Furthermore, it could be found that the feeding rate had an increase of 68-190% at the same range of $v_{g,in}$ by adding fluidizing gas at the flowrate of 6.1×10^{-4} kg/s, while the m_s/m_g had a decrease of 10%-17% according to the comparison of Figs. 3 and 5, and the feeding fluctuation decrease from 6.5% to 4%. Also, in comparing Fig. 6 with 4, one could noticed that an extra injection gas at the flowrate of 6.1×10^{-4} kg/s resulted in an increase of 200-750% and 73-285% on the feeding rate and m_s/m_g, respectively, at the same range of $v_{g,fl}$, but the feeding fluctuation did not change much.

Based on the above findings, it could be concluded that using injection gas would benefit the effciency of gas as a conveyance means. This was because the injection gas was running toward the feeding pipe, leading to lower pressure loss. On the other hand, using fluidizing gas caused lower fluctuation compared with the injection gas. It was due to the reduced possibilities of material bridging and agglomeration. Therefore, introducing fluidizing gas would improve the conveying continuity and stability.

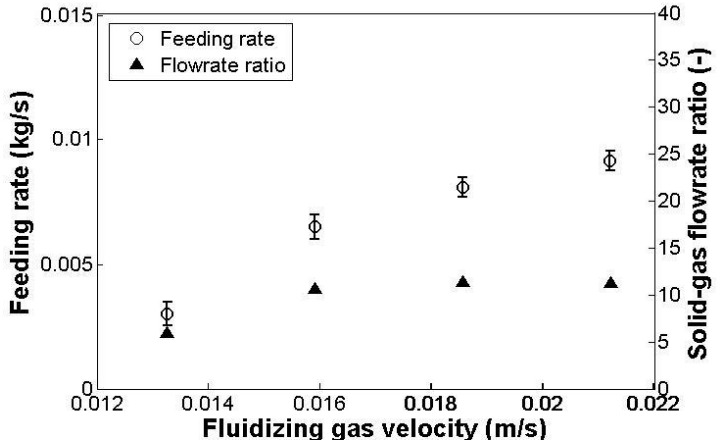

Fig. 4. Feeding rate as a function of fluidizing gas velocity ($m_{g,in}$ = 0, L = 50 mm, injection nozzle ID 9.5 mm, gas distributor A)

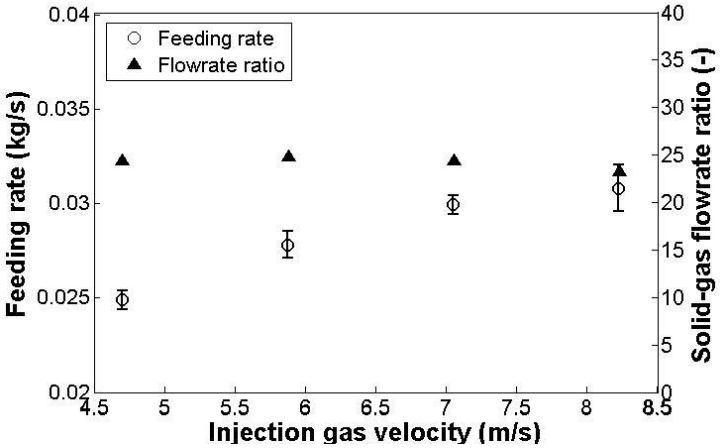

Fig. 5. Feeding rate as a function of injection gas velocity ($m_{g,fl}$ = 6.1 × 10^{-4} kg/s, L = 50 mm, injection nozzle ID 9.5 mm, gas distributor A)

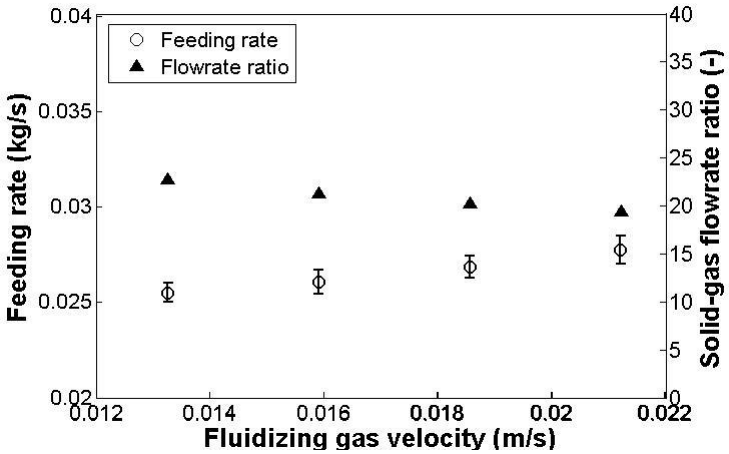

Fig. 6. Feeding rate as a function of fluidizing gas velocity ($m_{g,in}$ = 6.1 × 10^{-4} kg/s, L = 50 mm, injection nozzle ID 9.5 mm, gas distributor A)

Effect of Injection Pipe on Biomass Feeding

According to the above findings, using an injection gas to transport the biomass resulted in a higher solid to gas flowrate ratio compared with fluidizing gas, which revealed the effect of the injection pipe on kinetic energy saving. In this section, relationships between the feeding rate and the position of injection pipe and its ID were studied to demonstrate the role of the injection pipe in biomass feeding. As shown in Fig. 7, the distance from the injection pipe tip to the inlet of the feeding pipe was defined as an effective injection distance (*L*), which was an important parameter in biomass feeding. Keeping the injection gas flowrate to 5.1×10^{-4} kg/s , experiment using different injection pipes with various *L* was performed, and the result was presented in Fig. 8. It was shown that the injection pipe with a smaller ID led to a higher feeding rate when using the same injection gas flowrate. This was because the smaller ID injection pipe led to a higher gas velocity, and the gas velocity had a positive effect on the feeding rate, as indicated in Fig. 3. For the effective injection distance, it seemed that the shorter *L* would cause a higher feeding rate according to profiles of 13.5 and 16.5 mm ID. This was because the kinetic energy dissipation would increase with the travel distance of the gas. However, when the 9.5 mm ID injection pipe was used, the feeding rate increased at first and started to decline while *L* was lager than 50 mm. This was mainly because that the decrease in *L* would narrow the path for biomass particles entering the feeding pipe. As shown in Fig.7, the path for biomass could be represented by the flow field of injection gas inside the pressure chamber (dash line). The envelop surface area of the flow field was expressed as,

$$A = \frac{\pi}{\tan\beta}\left[\left(\frac{d_1}{2} + L\tan\beta\right)^2 - \frac{{d_1}^2}{4}\right] \quad (1)$$

where *A* was the envelop surface area of the flow field; β was the diffusion angle.

As could be seen, reducing both *L* and ID (d_1 in Fig.7) would lead to a decrease in *A*, which had an impact on biomass flowing into the feeding pipe. From this point of view to guarantee the space of solid movement, *L* must not be too short. As a result, an injection pipe with an ID = 9.5 mm was selected for the rest of the experiments.

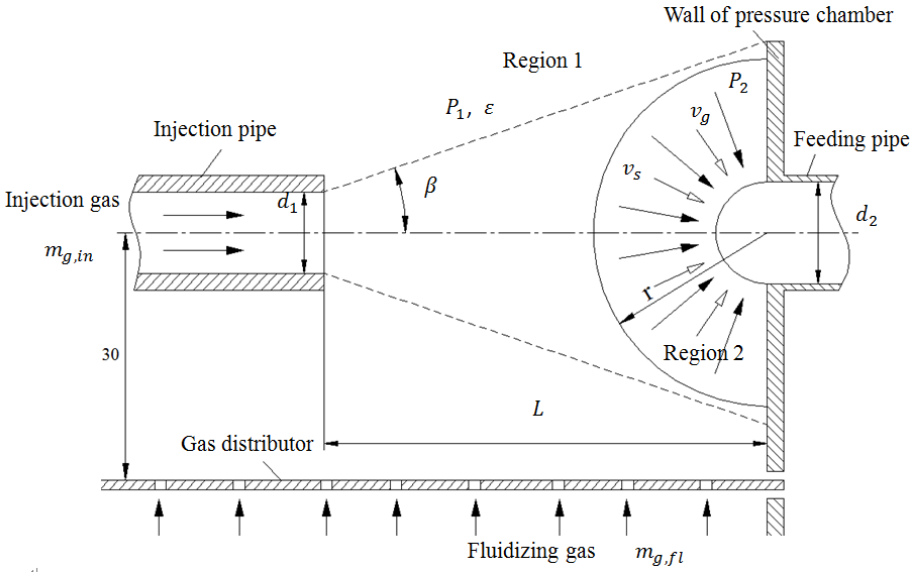

Fig. 7. Physical model of gas and solid flow inside the feeder

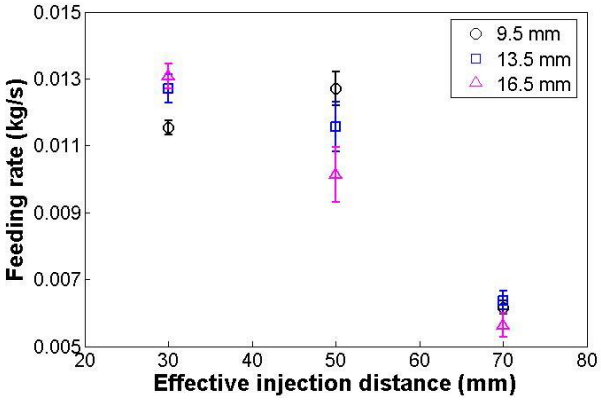

Fig. 8. Feeding rate as a function of effective injection distance using different injection pipes ($m_{g,in}$ = 5.1 × 10^{-4} kg/s, $m_{g,fl}$ = 0, gas distributor A)

Effect of a Gas Distributor on Biomass Feeding

Three different gas distributors were used to investigate their influence on the biomass conveying of this feeder. Because the holes of gas distributor C were non-uniformly arranged, it was used twice in this testing to deeply study its impact on the biomass conveying (case 1: dense part near the feeding pipe; case 2: dilute part near the feeding pipe). Experiments were performed using only the fluidizing gas. Thus, the feeding rate as a function of fluidizing gas velocity was plotted for each case. As shown in Fig. 9, the conveying using gas distributor A resulted in a higher feeding rate compared with that of B, which might be attributed to its larger opening ratio. However, a larger opening ratio also caused a higher standard deviation, which might have an impact on conveying stability.

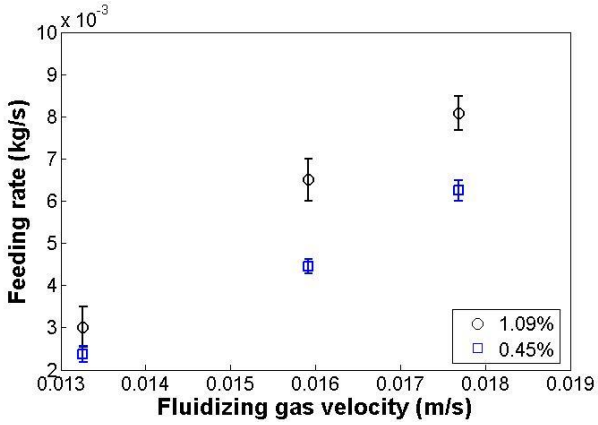

Fig. 9. Feeding rate as a function of fluidizing gas velocity using gas distributor A and B ($m_{g,in}$ = 0, L = 50 mm, injection pipe ID 9.5 mm)

Meanwhile, the performances of the two cases of gas distributor C were also presented, as shown in Fig. 10. It was indicated that the increase in the opening ratio near the feeding pipe would lead to a higher feeding rate. This was mainly because the flowrate in the dense part of gas distributor C was higher than that of the other part, which led to gas entering the feeding pipe easier in case 1. However, it seemed that feeding rates of both cases were higher than that of gas distributor A, though the opening ratio of gas distributor C was smaller than the former, and the reason needs to be found through further research. In general, the gas distributor with smaller opening ratio was preferred to guarantee the feeding continuity and stability in spite of the lower feeding rate.

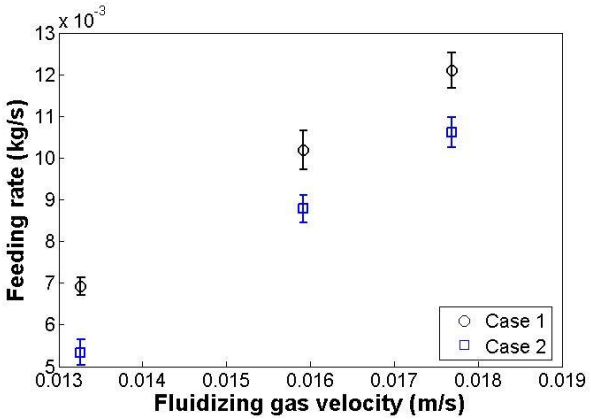

Fig. 10. Feeding rate as a function of fluidizing gas velocity using gas distributor C ($m_{g,in}$ = 0, L = 50 mm, injection pipe ID 9.5 mm)

Feeder Modeling

With the fundamental investigation of this new feeder, some basic information was obtained. Consequently, a model was needed to predict the biomass conveying characteristics for the successful feeder design. In general, the goal of the model was to predict the feeding rate with any given input data, which included the fluid and construction parameters.

The theory of Tallon, which described the gas and solids flow through an orifice at the side of the fluidized bed, was adopted to establish a simple one-dimensional flow model of this feeder (Tallon and Davies 2005). To do this, the volume of the pressure chamber and the feeding pipe were divided into two regions, as shown in Fig. 7. In region 1, the gas and particles would flow toward the feeding pipe due to the pressure gradient between the pressure chamber and the feeding pipe. In region 2, the pressure fell to zero and the particles became free to accelerate without restriction. Clearly, the mass flow rate of particles was determined by the pressure gradient in region 1, and the shape of the boundary of the two regions based on this theory. To simplify the model, some assumptions had to be made:

1) The effect of acceleration of gravity was ignored;
2) The void volume of biomass particles inside region 1 was assumed to be uniform throughout;
3) The boundary of region 1 and 2 was modeled as a hemispherical surface with a uniform radius (Fig. 7);
4) The gas velocity in region 1 remained constant;
5) The pressure in region 1 remained constant and was uniform in each run of experiment;
6) The mass of both gas and solid in region 1 and 2 was conserved during flowing;
7) The kinetic energy loss due to friction was ignored.

Based on the third assumption, the problem could then be reduced to one physical dimension defined by a hemispherical surface at distance r (m) from the center of the inlet of the feeding pipe. In this case, the pressure would only change in region 2. Clearly, it was the pressure gradient that caused a solid flow toward the feeding pipe. The Ergun equation

was used to describe the pressure drop in region 2 near the inlet of the feeding pipe, as given in Eq. 2,

$$\frac{dP_2}{dr} = \frac{150\mu_g(1-\varepsilon)^2}{{d_s}^2\varepsilon^2}(v_g - v_s) + \frac{1.75\rho_g(1-\varepsilon)}{d_s\varepsilon}(v_g - v_s)^2 \quad (2)$$

where, P_2 represented the gauge pressure in region 2 (Pa), v_g and v_s were the gas (m/s) and solid velocities (m/s) in region 2, ε was the void volume proportion of biomass particles and was close to the natural packing voidage of the biomass particles, μ_g and p_g were the viscosity (Pa • s) and density (kg/m^3) of the gas, and d_s was the particle diameter (m) of biomass and was represented by the mean particle diameter of the material used in this study.

Because the boundary of region 1 and 2 was a hemispherical surface, the velocities of gas and solid could be determined by their mass flow rates and distance r,

$$v_g = \frac{m_g}{\varepsilon\rho_g 2\pi \cdot r^2} \quad (3)$$

$$v_s = \frac{m_s}{(1-\varepsilon)\rho_s 2\pi \cdot r^2} \quad (4)$$

As shown in Eqs. 3 and 4, the gas and solid velocities were functions of the distance r. By using such equations, it also had to be assumed that both the gas and solid flowed steadily toward the inlet of the feeding pipe.

Apparently, the pressure in region 2 was dependent on the distance r, which could be written as the following expression, based on the Bernoulli equation,

$$P_2 = P_1 + \frac{\rho_g {v_1}^2}{2} - \frac{\rho_g {v_g}^2}{2} \quad (5)$$

Substituting Eq. 3 in Eq. 5, P_2 could be expressed as,

$$P_2 = P_1 + \frac{\rho_g {v_1}^2}{2} - \frac{\rho_g}{2}\left(\frac{m_g}{\varepsilon\rho_g 2\pi}\right)^2 \frac{1}{r^4} \quad (6)$$

where, P_1 and v_1 were the gas pressure (Pa • s) and mean gas velocity (m/s) in region 1 respectively, which were constants based on assumption 4 and 5. As a result, by taking the derivative of P_2 the following expression could be obtained,

$$\frac{dP_2}{dr} = 2\rho_g\left(\frac{m_g}{\varepsilon\rho_g 2\pi}\right)^2 \frac{1}{r^5} \quad (7)$$

Substituting Eqs. 3, 4, 6, and 7 in Eq. 2, Eq. 8 could be obtained,

$$\frac{300\pi\mu_g(1-\varepsilon)^2}{{d_s}^2\varepsilon^2}\left[\frac{m_g}{\varepsilon\rho_g} - \frac{m_s}{(1-\varepsilon)\rho_s}\right]r^3 + \frac{1.75\rho_g(1-\varepsilon)}{d_s\varepsilon}\left[\frac{m_g}{\varepsilon\rho_g} - \frac{m_s}{(1-\varepsilon)\rho_s}\right]^2 r - \frac{2{m_g}^2}{\varepsilon^2\rho_g} = 0 \quad (8)$$

Equation 8 could be seen as the equation where r was the unique independent if m_g and m_s were treated as constants. Using data in Fig. 4 to substitute m_g and m_s, r could be plotted as a function of $m_{g,fl}$, because there was no injection gas involved, and a linear relationship between r and $m_{g,fl}$ was observed, which was expressed as,

$$r = 24 m_{g,fl} \quad (9)$$

where, $m_{g,fl}$ represented the mass flow rate of the fluidizing gas, and R^2 was 0.991, which showed a remarkable correlation between r and $m_{g,fl}$.

Similarly, using the data in Fig. 3, one could also obtain a linear correlation between r and $m_{g,in}$,

$$r = 32 m_{g,in} \tag{10}$$

where, $m_{g,in}$ was the mass flow rate of the injection gas (kg/s), and R^2 was 0.981.

However, Eqs. 9 and 10 applied to cases where only the fluidizing or injection gas was used. In fact, the gas mass flow rate in region 1 and 2 was the sum of the fluidizing and injection gas, and it was further assumed that the source of gas would not affect the pressure in region 1 and 2, but would affect *r*. Therefore, it was reasonable to replace m_g and *r* in Eq. 8 with the following expressions to predict the feeding rate of the feeder when both the fluidizing and injection gas were used,

$$m_g = m_{g,fl} + m_{g,in} \tag{11}$$

$$r = 24 m_{g,fl} + 32 m_{g,in} \tag{12}$$

To verify this model, more experiments were performed to test the mass flow rate through the feeding pipe using the fluidizing and injection gas together. By solving Eqs. 8, 11, and 12, the mass flow rate under different $m_{g,fl}$ and $m_{g,in}$ could be obtained. The comparison of feeding rates obtained *via* experiment and prediction is shown in Fig. 11. The model had an error of ± 5%, which was accurate enough to predict the feeding rate of the feeder with certain construction parameters.

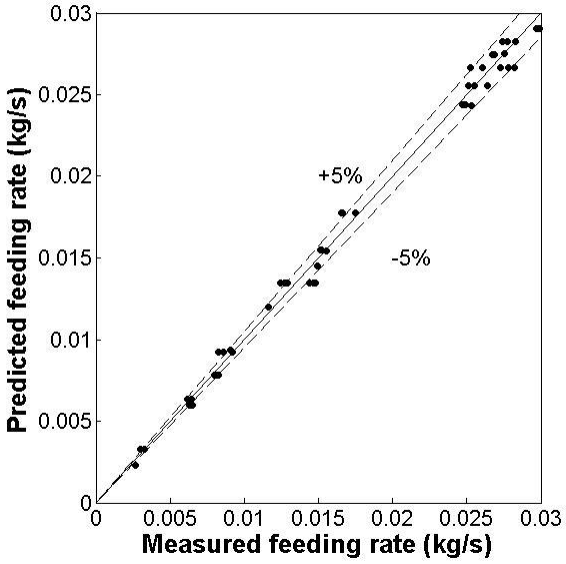

Fig. 11. Comparison of feeding rates obtained by the experiment, and prediction without effects of construction parameters

It was noteworthy to emphasize that the current model was only suitable for a 9.5 mm ID injection pipe with L = 50 mm when the injection gas was used. According to the above findings, construction parameters of the feeder (ID of the injection pipe and *L*) had remarkable influences on the feeding rate as indicated in Fig. 8, which could have been attributed to their effects on *r*. To derive a correlation between *r* and the construction parameters, Eq. 10 was modified as follows,

$$r = f(d_1, L) m_{g,in} \tag{13}$$

Two non-dimensional parameters were defined to replace d_1 and L in Eq. 13, $\frac{d_1}{D}$ and $\frac{L}{D}$, where D is the diameter of the pressure chamber. Based on the present knowledge, both d_1 and L had negative effects on the feeding rate; therefore Eq. 13 was further modified as follows,

$$r = s \cdot \frac{D^2}{d_1 L} m_{g,in} \tag{14}$$

where s was set as a temporary coefficient. By substituting Eq. 14 in Eq. 8, the relationship between s and $\frac{d_1}{D}$, $\frac{L}{D}$ was obtained. Using data in Fig. 8 where $m_{g,in}$ was a constant, an expression of s could be derived through a regression analysis, where powers of $\frac{d_1}{D}$, $\frac{L}{D}$ and $\frac{d_1 L}{D^2}$ were considered as independents, such as $\left(\frac{d_1}{D}\right)^2$ and $\left(\frac{d_1}{D}\right)^{-1}$.

It was found that $\left(\frac{L}{D}\right)^2$ and $\frac{d_1 L}{D^2}$ had more remarkable effects on s compared with other ones, and the regression model was written as Eq. 15, with $R^2 = 0.998$.

$$s = 15.5\frac{d_1 L}{D^2} - 0.19\left(\frac{L}{D}\right)^2 + 0.02 \tag{15}$$

As a result, Eq. 12 could be modified as the following expression,

$$r = 24 m_{g,fl} + \left(15.5 - 0.19\frac{L}{d_1} + 0.02\frac{D^2}{d_1 L}\right) m_{g,in} \tag{16}$$

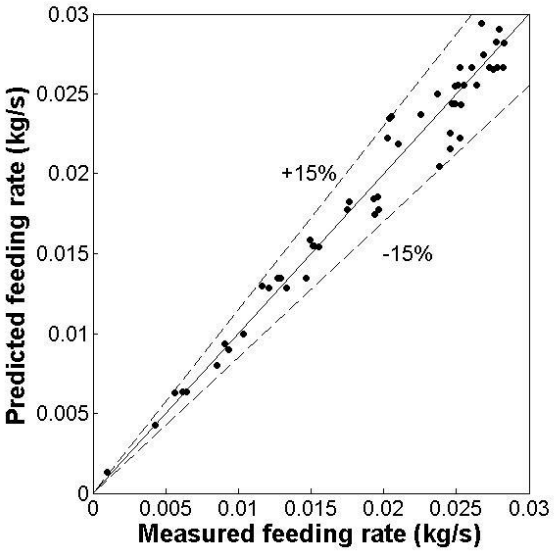

Fig. 12. Comparison of feeding rates obtained by experiment and prediction including effects of construction parameters

By combining Eq. 16 with 8, the feeding rates under different d_1, L, and velocities of the fluidizing and injection gas could be calculated. To verify the model, the calculated

values were compared with more experimental data that used three injection pipes with different IDs. As shown in Fig. 12, the error did not exceed ± 15%, which established the model's capability of predicting the feeding rate of the dual pneumatic feeder.

The developed model was suitable for feeding rate prediction when gas distributor B (opening ratio 0.45%) was used. However, only three injection pipes were considered in this study. Also, the suitable ranges for injection and fluidizing gas velocities were 4.5 m/s to 8.5 m/s and 0.012 m/s to 0.022 m/s, respectively. Because the model was developed to describe the relationship of the feeding rate and the construction parameters of the feeder, many more experiments, considering the effects of the injection pipe and gas distributor, should be performed for future research on the topic.

CONCLUSIONS

1. A new dual pneumatic feeder to convey biomass particles for pyrolysis was proposed. An injection pipe was installed inside the pressure chamber, which was full of feedstock to facilitate feedstock replenishing, and a gas distributor was also used to fluidize the feedstock to prevent bridging.
2. Both injection and fluidizing gas velocities had positive effects on the feeding rate. The principle of improving the solid-gas flowrate ratio in a horizontal pipe was to increase the gas flow rate until all solids were suspended in the moving gas. It was also indicated that using injection gas would increase the effciency of gas, while using fluidizing gas would cause lower fluctuation, leading to a higher conveying continuity and stability.
3. The injection pipe with a smaller ID led to a higher feeding rate, while the effective injection distance had a negative impact on the feeding rate within a certain range. Although increasing opening ratio of the gas distributor would increase the feeding rate, it also caused higher fluctuation.
4. A mathematical model was developed based on the Ergun equation to describe the relationships between feeding rate and gas velocities, and the injection pipe ID and the efficient injection distance. The model had an error of ± 15% according to the comparison of predicted values and experimental data.

ACKNOWLEDGMENTS

The authors would like to express their sincerest gratitude to the Fundamental Research Funds for the Central Universities (BLYJ201515) and the 948 project of State Forestry Administration of the People's Republic of China (2012-4-19) for providing financial support for this study.

REFERENCES CITED

Annamalai, K., Ruiz, M., and Vo, N. (1992). "Locally fluidzing feeder for powder transport," *Powder Technol.* 73, 181-190. DOI: 10.1016/0032-5910(92)80079-C

Campbell, W. A., Fonstad, T., Pugsley, T., and Gerspacher, R. (2012). "MBM fuel feeding system design and evaluation for FBG pilot plant," *Waste Manage* 32(6), 1138-1147. DOI: 10.1016/j.wasman.2012.01.010

Dai, J., Cui, H., and Grace, J. R. (2012). "Biomass feeding for thermochemical reactors," *Prog. Energ. Combust. Sci.* 38(5), 716-736. DOI: 10.1016/j.pecs.2012.04.002

Luo, Y., Guda, V. K., Hassan, E. B., Steele, P. H., Mitchell, B., and Yu, F. (2016a). "Hydrodeoxygenation of oxidized distilled bio-oil for the production of gasoline fuel type," *Energy Conversion and Management* 112, 319-327. DOI: 10.1016/j.enconman.2015.12.047

Luo, Y., Street, J., Steele, P., Entsminger, E., and Guda, V. (2016b). "Activated carbon derived from pyrolyzed pinewood char using elevated temperature, KOH, H_3PO_4, and H_2O_2," *Bioresources* 11(4), 10433-10447. DOI: 10.15376/biores.11.4.10433-10447

Massimilla, L., Betta, V., and Rocca, C. D. (1961). "A study of streams of solids flowing from solid-gas fluidized beds," *AICHE J.* 502-508. DOI: 10.1002/aic.690070332

Pugsley, T. S., Milne, B.J., and Berruti, F. (1996). "An innovative non-mechanical solids feeder for high solids mass fluxes in circulating fluidized bed risers," *Powder Technol*. 88, 123-131. DOI: 10.1016/0032-5910(96)03118-X

Suri, A., and Horio, M. (2009). "A novel cartridge type powder feeder," *Powder Technol.* 189(3), 497-507. DOI: 10.1016/j.powtec.2008.08.001

Tallon, S., and Davies, C. E. (2005). "Discharge of a fluidised bed of particles through an orifice," *Powder Technol.* 160(1), 45-53. DOI: 10.1016/j.powtec.2005.04.050

Watson, R. J., Thorpe, R. B., and Davidson, J. F. (2012). "Vertical plug-flow pneumatic conveying from a fluidised bed," *Powder Technol.* 224, 155-161. DOI: 10.1016/j.powtec.2012.02.045

Wen, C. -Y., and Simon, H. P. (1959). "Flow characteristics in horizontal fluidized solids transport," *AICHE J* 5(2), 263-267. DOI: 10.1002/aic.690050225

Woods, J. A., Thorpe, R. B., and Johnson, S. E. (2008). "Horizontal pneumatic conveying from a fluidized bed," *Chem. Eng. Sci.* 63(7), 1741-1760. DOI: 10.1016/j.ces.2007.11.040

Wypych, P. W. (1999). "Pneumatic conveying of powders over long distances and at large capacities," *Powder Technol.* 104, 278-286. DOI: 10.1016/S0032-5910(99)00105-9

Wypych, P. W., and Yi, J. L. (2003). "Minimum transport boundary for horizontal dense-phase pneumatic conveying of granular materials," *Powder Technol.* 129(1-3), 111-121. DOI: 10.1016/S0032-5910(02)00224-3

Article submitted: January 21, 2017; Peer review completed: March 30, 2017; Revised version received and accepted: April 4, 2017; Published: July 5, 2017.
DOI: 10.15376/biores.12.3.5970-5983